Ann. Rev. Nucl. Part. Sci. 1985. 35 : 245–70

THE TRANSITION FROM HADRON MATTER TO QUARK-GLUON PLASMA

H. Satz

Fakultät für Physik, Universität Bielefeld, D-4800 Bielefeld, West Germany

CONTENTS

INTRODUCTION

During the past two decades, our concept of an elementary particle has undergone a fundamental change. We now understand hadrons as bound states of quarks, and thus as composite. In strong interaction physics, quarks have become the smallest building blocks of nature. But the binding force between quarks increases with the distance of separation, making it impossible—as far as we know today—to split a given hadron into its quark constituents. If we insist on individual existence, the hadron remains elementary.

This modification of our hadron picture has led to remarkable consequences in strong interaction thermodynamics: at high density, nuclear matter must become a quark plasma. In return, strong interaction

0163–8998/85/1201–0245$02.00

thermodynamics has shown us the limits of quark confinement: in sufficiently dense matter, quarks can become free.

Such high densities prevailed in the very early universe, until about 10^{-6} seconds after the big bang; only then were quarks confined to form hadrons. To create and study such a primordial plasma in the laboratory is one of the great challenges for current experimental physics. Various estimates (e.g. 1) indicate that the collision of heavy nuclei at very high energies may indeed produce a terrestrial "little bang," providing short-lived bubbles of the quark-gluon plasma. First experiments toward this ultimate goal are expected to start in the summer of 1986, using existing accelerators at Brookhaven National Laboratory and at CERN. A dedicated large-scale machine for this purpose was recently proposed (2).

Phenomenological indications for critical behavior in strong interaction thermodynamics were first seen quite early (3). However, these considerations were based on the dynamics of elementary hadrons and thus could only indicate at what point the resulting statistical mechanics was expected to break down; they said nothing about what might happen beyond that point. The advent of the quark model suggested a new state of matter, and quantum chromodynamics (QCD) supplied the theoretical basis for a two-phase picture of strongly interacting systems.

The perturbative evaluation of QCD at small coupling leads to an equation of state for the quark-gluon plasma in the high-density limit (e.g. 4). It breaks down at sufficiently low densities—a result that has also been taken as an indication for critical behavior (5, 6). In this approach, it is the low-density regime that remains unattainable.

To cover the entire density range of strong interaction thermodynamics, a nonperturbative evaluation method for QCD is necessary. The lattice formulation (7) provides the basis for such a method—so far, the only one we have. It leads to a partition function whose form is that of a generalized spin system and which can therefore be dealt with by methods developed in statistical physics.

In lattice QCD, the existence of a deconfined phase is now rigorously established (8). First indications for a deconfinement transition had in this context been obtained in the strong coupling approximation (9a,b). The real breakthrough occurred, however, when it became clear that the lattice formulation of QCD could be evaluated by computer simulation (10). After initial studies of the confining potential, this method was quickly extended and applied to gauge field thermodynamics (11–13). Today, it is used extensively in studying the phase structure and the features of strongly interacting matter as they are predicted by QCD.

The first part of this article is an introduction to the conceptual basis of critical phenomena in strongly interacting matter and to the formulation of

statistical quantum chromodynamics. In the second part, we summarize the results so far obtained in the lattice evaluation of QCD thermodynamics and attempt to assess their reliability. The final part presents some particularly interesting open questions as well as a few comments on the present status of the experimental attempts to study strong interaction thermodynamics.

STATISTICAL QUANTUM CHROMODYNAMICS

The Gauge Field Theory of Strong Interactions

Quantum chromodynamics (QCD) describes the interaction of quarks and gluons in the form of a gauge field theory, very similar to quantum electrodynamics (QED) of electrons and photons. In both cases we have spinor matter fields interacting through massless vector gauge fields. In QCD, however, the intrinsic color charge is associated with the non-Abelian gauge group SU(3), in place of the Abelian group U(1) for the electric charge in QED. The quarks thus carry three color charges, and the gluons, transforming according to the adjoint representation, carry eight. The intrinsic charge of the gauge field is the decisive modification in comparison to QED; it makes the pure gluon system directly self-interactive, in contrast to the ideal gas of photons. As a result, the three-dimensional Laplace equation, which in nonrelativistic QED leads to the Coulomb potential $V \sim 1/r$, becomes effectively one-dimensional for massive quarks, with the confining potential $V \sim r$ as the solution.

The Lagrangian density of QCD is given by

$$\mathcal{L} = -\tfrac{1}{4}F^a_{\mu\nu}F^{\mu\nu}_a - \sum_f \bar{\psi}^f_\alpha (i\partial\!\!\!/ - g A\!\!\!/)^{\alpha\beta}\psi^f_\beta, \qquad 1.$$

with

$$F^a_{\mu\nu} = (\partial_\mu A^a_\nu - \partial_\nu A^a_\mu - g f^a_{bc} A^b_\mu A^c_\nu). \qquad 2.$$

Here A^a denotes the gluon field of color a ($a = 1, \ldots, 8$) and ψ^f_α the quark field of color α ($\alpha = 1, 2, 3$) and flavor f. We restrict ourselves here to the effectively massless u and d quarks, which suffice to form all nonstrange mesons and baryons. Strange and exotic quarks are much more massive and hence thermodynamically suppressed at finite temperatures. The inclusion of quark masses would add a term

$$\mathcal{L}_m = \sum_f m_f \bar{\psi}^f_\alpha \psi^{\alpha,f} \qquad 3.$$

in Equation 1. The structure functions f^a_{bc} are fixed by the color gauge group, whose generators we denote by λ_a; with them, we define $A = A^a\lambda_a/2$

in Equation 1. The generators satisfy

$$[\lambda_a, \lambda_b] = if^c_{ab}\lambda_c. \qquad 4.$$

If we would set $f = 0$, the Lagrangian density (Equation 1) would simply reduce to that of QED, as there would then be no self-interaction among the gluons.

Equation 1 contains one dimensionless coupling constant, g, and hence provides no scale. The resulting invariance under scale transformations implies that QCD predicts only the ratios of physical quantities, not absolute values in terms of physical units.

In QCD, hadrons are color-neutral bound states of quarks or of quark-antiquark pairs; they are thus the chromodynamic analogue of atoms of positronium as the electrically neutral states in QED. In both cases is the binding radius determined as the point at which the attractive potential just balances the kinetic energy required by the momentum uncertainty at that spatial localization. The difference between the two theories becomes most significant at large distances: while a finite ionization energy ΔE suffices to break the electrodynamic bond, this is not possible in the case of quark binding.

As the fundamental theory of strong interactions, QCD must then predict the ratios of all hadron masses as well as describe hadronic scattering processes. The successful application of perturbative QCD to scattering at large momentum transfer was decisive in establishing it as the basic theory (e.g. 14). The hadronic mass spectrum is presently under intensive investigation, and calculations seem to be well on the way toward definitive results (e.g. 15). Here we take QCD as the dynamical input needed for the statistical description of strongly interacting matter.

The Physical Basis for Deconfinement

For composite hadrons of nonvanishing spatial extension, the concept of hadronic matter appears to lose its meaning at sufficiently high density. Once we have a system of mutually interpenetrating hadrons, each quark finds in its immediate vicinity, at a distance of less than a hadron radius, many other quarks. There does not seem to be a way for a given quark to identify those other quarks which at lower density were its partners in some specific hadron, and we should therefore now consider the system as quark matter.

The mechanism for the deconfinement of quarks in dense matter is provided by the screening of their color charge (9b, 16). In dense atomic matter, the long-range Coulomb potential that binds ions and electrons into electrically neutral units is partially screened by the other charges

present and thus becomes of much shorter range,

$$e_0^2/r \to (e_0^2/r)\exp(-r/r_D). \quad 5.$$

Here r denotes the distance from the probe to the charge e_0. The Debye screening radius r_D is inversely proportional to the charge density n,

$$r_D \sim n^{-1/3}. \quad 6.$$

Hence, at sufficiently high density, r_D will become smaller than the atomic binding radius r_A. A given electron can now no longer feel the binding force of "its" ion and it is therefore set free; at this point, insulating matter becomes electrically conductive (17). We expect deconfinement to be the chromodynamic analogue of this Mott transition. Since screening is a phenomenon occurring at high density and hence at short range, the difference between electrodynamic and chromodynamic forces at large r here is not important. Moreover, the decrease of the color charge with increasing density, resulting from asymptotic freedom (e.g. 18), further enhances the deconfinement.

The color conductivity of strongly interacting matter thus constitutes a rather natural signal for the deconfinement transition: it should vanish for normal hadronic matter as the color insulating state and become nonzero when the system turns into a plasma and hence a color conductor. In insulating solids, however, the electric conductivity σ_e for $T > 0$ is not strictly zero, but only exponentially small (17),

$$\sigma_c \sim \exp(-\Delta E/T), \quad 7.$$

with ΔE denoting the ionization energy. Above the Mott transition temperature, σ_e is significantly nonzero because Debye screening has globally dissolved the Coulomb binding between ions and electrons, but even below this point, thermal ionization can locally produce some few free electrons, making σ_e small but nonzero. The corresponding phenomenon in QCD is the production of a quark-antiquark pair in form of a hadron (19). If we try to remove a quark from a given hadron, the confining potential will rise with the distance of separation until it reaches the value m_H of the lowest $q\bar{q}$ state; at this point, an additional hadron will form, whose antiquark neutralizes the quark we were trying to remove, and the separation thus becomes possible. Local hadron production therefore plays the role of ionization, and we expect that the color conductivity σ_c will not vanish in the confinement regime, but instead be given by

$$\sigma_c \sim \exp(-m_H/2T), \quad 8.$$

where m_H is the mass of the lowest $q\bar{q}$ state. Both electric and color

conductivity should vanish identically at $T = 0$. In the chromodynamic case, however, we can let $m_H \to \infty$ and consider the thermodynamics of a pure gauge field system. In this case, we expect from Equation 8

$$\sigma_c \begin{cases} = 0 & T \leq T_c \\ > 0 & T > T_c \end{cases}, \qquad 9.$$

so that here σ_c should vanish in the entire confinement regime and thus form a true order parameter for the deconfinement transition.

Lattice QCD at Finite Temperature

With the Lagrangian density (Equation 1) provided, the formulation of statistical QCD becomes, at least in principle, a well-defined problem. We have to calculate the partition function

$$Z(\beta, V) = \mathrm{Tr}\{e^{-\beta H}\}. \qquad 10.$$

In the trace we have to sum over all physical states accessible to a system in a spatial volume V; $\beta^{-1} = T$ denotes the physical temperature. Once $Z(\beta, V)$ is obtained, we can calculate all thermodynamic observables in the canonical fashion; thus

$$\varepsilon = (-1/V)(\partial \ln Z/\partial\beta)_V \qquad 11.$$

gives us the energy density, and

$$P = (1/\beta)(\partial \ln Z/\partial V)_\beta \qquad 12.$$

give us the pressure.

In practice, the evaluation of statistical QCD encounters two main obstacles. Perturbative calculations lead to the usual divergences of quantum field theory; we thus have to renormalize to obtain finite results. Moreover, we want to study the entire range of behavior of the system, from confinement to asymptotic freedom—i.e. for all values of the coupling. That is not possible perturbatively; we need a new approach for the solution of a relativistic quantum field theory. It is provided by the lattice regularization (7). Evaluating the partition function on a large but finite lattice whose points are separated by multiples of some spacing a, we have $1/a$ as largest and $1/(Na)$ as smallest possible momentum; here Na is the linear lattice size. Hence neither ultraviolet nor infrared divergences can occur at finite N and nonzero a. We are left with two questions, however: how can we ensure that physical observables are independent of this regularization, and how can we actually carry out calculations? Renormalization group theory answers, as we discuss below, the first of these questions. The Monte Carlo simulation of the lattice form of statistical QCD then allows us to carry out

calculations of thermodynamic observables at any coupling—thus answering the second question.

The lattice formulation of statistical QCD is obtained in three steps. First we replace the Hamiltonian form (Equation 10) of the partition function by the corresponding Euclidean functional integral (20)

$$Z_E(\beta, V) = \int (dA\ d\psi\ d\bar{\psi}) \exp\left[-\int_V d^3x \int_0^\beta d\tau\ \mathcal{L}(A, \psi, \bar{\psi}) \right]. \qquad 13.$$

This form involves directly the Lagrangian density, and by integrating over field configurations, we avoid having to project onto the allowed physical states in the trace (Equation 10). The spatial integration over $\mathcal{L}$ is performed over the entire volume of the system, which in the thermodynamic limit becomes infinite, while in the imaginary time $\tau \equiv ix_0$, the integration runs over a finite slice determined by the temperature. The finite temperature behavior of the partition function thus becomes a finite size effect in the integration over τ. Equation 13 is obtained from the trace form in Equation 10. As a consequence, the vector (spinor) fields have to be periodic (antiperiodic)

$$\begin{aligned} A(\mathbf{x}, \tau = 0) &= A(\mathbf{x}, \tau = \beta), \\ \psi(\mathbf{x}, \tau = 0) &= -\psi(\mathbf{x}, \tau = \beta), \\ \bar{\psi}(\mathbf{x}, \tau = 0) &= -\bar{\psi}(\mathbf{x}, \tau = \beta), \end{aligned} \qquad 14.$$

at the boundaries of the imaginary time integration.

Next, the Euclidean $\mathbf{x}-\tau$ manifold is replaced by a discrete lattice, with N_σ points and lattice spacing a_σ in each space direction, and N_τ points and spacing a_τ for the τ axis. The overall space volume thus becomes $V = (N_\sigma a_\sigma)^3$, the inverse temperature $\beta^{-1} = N_\tau a_\tau$. The spin quark fields ψ and $\bar{\psi}$ are now defined on each of the $N_\sigma^3 N_\tau$ lattice sites. To ensure the gauge invariance of the formulation, the gauge fields A must, however, be defined on the links connecting each pair of adjacent sites (21).

In the final step, the integration over the gluon fields is replaced by one over the corresponding gauge group variables

$$U_{ij} \equiv \exp\left[-ig(x_i - x_j)^\mu A_\mu\left(\frac{x_i + x_j}{2}\right)\right], \qquad 15.$$

with x_i and x_j denoting two adjacent lattice sites; thus U_{ij} is an SU(3) matrix associated to the link between these two sites.

The QCD partition function thus becomes on the lattice

$$Z(N_\sigma, N_\tau; g^2) = \int \prod_{\text{sites}} d\psi_i\, d\bar{\psi}_i \prod_{\text{links}} dU_{ij} \exp\left[-S(\bar{\psi}, \bar{\psi}, U)\right], \qquad 16.$$

a form somewhat reminiscent of the partition function of a spin system, with ψ, $\bar{\psi}$, and U in place of the spin configurations. The QCD action S in the Wilson formulation (7) has the form

$$S = S_G + S_Q, \tag{17.}$$

with (13)

$$S_G = \frac{6}{g_\sigma^2}\frac{a_\tau}{a_\sigma}\sum_{P_\sigma}(1-\tfrac{1}{3}\text{Re Tr } UUUU) + \frac{6}{g_\tau^2}\frac{a_\sigma}{a_\tau}\sum_{P_\tau}(1-\tfrac{1}{3}\text{Re Tr } UUUU) \tag{18.}$$

for the action corresponding to the pure gauge field term $F^a_{\mu\nu}F^{\mu\nu}_a$ of the Lagrangian density (Equation 1). It contains two distinct coupling parameters, g_σ and g_τ; these are necessary as long as we consider the spatial and temporal lattice spacings a_σ and a_τ as independent variables (22). If we set $a_\sigma = a_\tau \equiv a$, then, we recover one "isotropic" coupling

$$g_\sigma(a) = g_\tau(a) \equiv g. \tag{19.}$$

The actual form of the action S_G is that of a generalized, gauge-invariant Ising model (21). For the usual Ising model, we have a lattice sum over the interactions of next-neighbor spins,

$$S_I \sim \sum_{\substack{\text{next neighbors}\\(i,j)}} (1-s_i s_j). \tag{20.}$$

In Equation 18, the spin variables s_i are generalized to the SU(3) color group matrices U, and in order to maintain gauge invariance, the product of next-neighbor spins is replaced by that over the four "spins" around the smallest possible closed path in the lattice ("plaquette"). The two terms of Equation 18 thus denote summations over space-space and space-time plaquettes, respectively.

The quark action S_Q in the Wilson formulation of Equation 1 is given by

$$S_Q = \sum_f \bar{\psi}_f(1-\kappa M)\psi_f, \tag{21.}$$

where the interaction matrix M depends on direction:

$$M_{\mu,nm} = (1-\gamma_\mu)U_{nm}\delta_{n,m-\hat{\mu}} + (1+\gamma_\mu)U^+_{mn}\delta_{n,m+\hat{\mu}}. \tag{22.}$$

Here $\hat{\mu}$ is a unit vector along the lattice link in the μ direction. The quark coupling strength, the "hopping parameter" κ, at finite temperature also

depends on the link direction, just as g does. The scalar product κM is

$$\kappa M \equiv \kappa_\tau M_0 + \kappa_\sigma \sum_{\mu=1}^{3} M_\mu. \qquad 23.$$

The hopping parameter also reduces to one variable for $a_\sigma = a_\tau \equiv a$:

$$\kappa_\tau(a) = \kappa_\sigma(a) = \kappa. \qquad 24.$$

Since the basic Lagrangian in Equation 1 contains only one coupling, the introduction of a separate quark coupling is a lattice artifact; κ must in principle be expressible in terms of g. For massless quarks we have in fact (23)

$$\kappa(g) = \tfrac{1}{8}[1 + 0.11g^2 + O(g^4)] \qquad 25.$$

for sufficiently small g^2.

With Equations 16–18, 21, and 22, we have a completely defined lattice formulation for the QCD partition function. It gives us $Z[N_\sigma, N_\tau, g = (g_\tau, g_\sigma)]$. To obtain the desired physical partition function $Z(\beta, V)$ and the resulting thermodynamic observables, we choose $a_\sigma = a_\tau$ (of course, after carrying out differentiations such as needed in Equations 11 or 12). The coupling g can then be related to the lattice spacing a by the asymptotic renormalization group relation

$$a\Lambda_L = \exp\left\{-\frac{4\pi^2}{(33-2N_f)}\left(\frac{6}{g^2}\right) + \frac{459-57N_f}{(33-2N_f)^2}\log\left[\frac{8\pi^2}{(33-2N_f)}\left(\frac{6}{g^2}\right)\right]\right\}, \qquad 26.$$

with the following reasoning. We want our lattice formulation to provide results independent of the specific lattice used in the evaluation. Renormalization group considerations assure us that this is the case in the vicinity of the fixed point $g = 0$; if coupling g and lattice spacing a are related through the equation

$$a\, \mathrm{d}g(a)/\mathrm{d}a = B(g), \qquad 27.$$

for $g \to 0$, we then recover the continuum theory. Here $B(g)$ is a function of g only; for small g it can be determined in a perturbation expansion, leading to Equation 26, with Λ_L as a dimensional integration constant. In quantitative studies, we must ascertain that at the coupling values used, this solution is indeed valid; although some deviations occur, this seems to be the case for the larger lattices presently used in numerical work (24). With $a(g)$ given by Equation 26, we then have $V = (N_\sigma a)^3$ and $\beta = (N_\tau a)$; this yields $Z(\beta, V)$ from Equation 16 for given N_σ, N_τ, and g.

All physical quantities are through Equation 26 measured in units of the

lattice scale Λ_L. As mentioned, the Lagrangian (Equation 1) contains no dimensional parameter, and hence Λ_L is arbitrary. We can thus either consider dimensionless ratios of observables, or calculate a specific quantity, such as the proton or ρ meson mass, to fix Λ_L in physical units.

To what extent now is this lattice formulation of statistical QCD equivalent to the continuum form of Equation 13? By letting $a = (x_i - x_j)$ in Equation 15 and subsequently go to zero, we recover the continuum formulation, Equation 13. The converse is not true, however: neither the gluon action (Equation 18) nor the quark action (Equation 22) are unique; various other forms have been considered, which give the same continuum limit (25–31). All physical results should, of course, be independent of the specific choice of action, and finite temperature thermodynamics provides a particularly sensitive test of this "universality." So far, it appears to be quite well satisfied (32).

The quark action leads to some additional problems. If we simply put fermions on the lattice by associating a spinor field with each lattice site, then the derivative in the Lagrangian (Equation 1) leads to the appearance of sixteen degenerate fermions per flavor (7, 30). To avoid this species doubling, Equation 22 gives fifteen of these quarks a mass m, with $m \to \infty$ in the continuum limit. Such a procedure, however, also has its difficulties. The continuum Lagrangian (Equation 1) for massless quarks is invariant under chiral transformations (18): massless fermions decompose into independent left-handed and right-handed particles. This invariance is broken in Wilson's lattice form Equations 21 and 22; it is recovered only in the continuum limit. It can in fact be shown (33) that the lattice formulation for massless fermions leads to species doubling, to chiral symmetry breaking, or to nonlocal derivatives. The choice of action thus is to some extent dictated here by the problem under investigation. And it is all the more important to check if all formulations lead to the same results.

THE COMPUTER SIMULATION OF STATISTICAL QCD

In the preceding section we saw that the lattice formulation of statistical QCD provides a partition function quite similar to that of a generalized spin system. Because even simpler spin systems, such as the three-dimensional Ising model, so far have not been solved analytically, it is not surprising that we also have to take recourse to the standard evaluation method for statistical systems—computer simulation. The advent of modern supercomputers has made the simulation of statistical QCD possible for quite large lattices. Here, as in many other areas of statistical physics (e.g. 34), computer experiments constitute a viable method of

obtaining quantitative predictions for systems with many degrees of freedom.

We noted above that the interaction decisive for confinement is contained in the pure gauge field part of the Lagrangian (Equation 1). Gauge field thermodynamics, without quarks, therefore provides a meaningful model for studying the deconfinement transition. As it also imposes less severe computer requirements and avoids the difficulties encountered in the lattice formulation of quarks, it was the first case to be taken up. We follow this order of development and begin with the thermodynamics of SU(N) gauge fields; to compare the critical behavior of spin and gauge systems, it is of interest to keep N general here. After that, we go on to include dynamical quarks.

Gauge Field Thermodynamics

The partition function for the SU(N) gauge field system on the lattice is given by (13)

$$Z(N_\sigma, N_\tau, g^2) = \int \prod_{\text{links}} dU \exp[-S_G(U)], \qquad 28.$$

with

$$S_G(U) = \frac{2N}{g_\sigma^2} \xi^{-1} \sum_{P_\sigma} \left(1 - \frac{1}{N} \text{Re Tr } UUUU\right) + \frac{2N}{g_\tau^2} \xi \sum_{P_\tau} \left(1 - \frac{1}{N} \text{Re Tr } UUUU\right). \qquad 29.$$

Here $\xi \equiv a_\sigma/a_\tau$; for $N = 3$, we recover Equation 18. For the energy density (Equation 11), we obtain

$$\varepsilon/T^4 = 6NN_\tau^4[g^{-2}(\bar{P}_\sigma \quad \bar{P}_\tau) + c_\sigma'(\bar{P} \quad \bar{P}_\sigma) + c_\tau'(\bar{P} - \bar{P}_\tau)], \qquad 30.$$

with $\bar{P}_\sigma$ and $\bar{P}_\tau$ denoting the lattice average of space-space and space-time plaquettes, respectively:

$$\bar{P}_\sigma = (3N_\sigma^3 N_\tau Z)^{-1} \int \prod_{\text{links}} dU \exp[S_G(U)] \left[\sum_{P_\sigma} \left(1 - \frac{1}{N} \text{Re Tr } UUUU\right)\right], \qquad 31.$$

and similarly for $\bar{P}_\tau$. The Euclidean form of the partition function differs from the Hamiltonian version by a normalizing factor corresponding to the $T = 0$ contribution (20). To take this into account, we have subtracted in Equation 30 from $\bar{P}_\sigma$ and $\bar{P}_\tau$ the plaquette average $\bar{P}$ calculated on a large symmetric lattice, of size N_σ^4 or larger; for the values of N_σ usually considered, it gives a good approximation of the zero-point contribution.

The constants c'_σ and c'_τ in Equation 30 arise from the differentiation of the couplings g_σ and g_τ with respect to the temperature; they have been calculated explicitly (35).

Returning for a moment to the structure of Equation 30, we note that the energy density of the gauge field system is obtained from plaquette averages, i.e. from the lattice average of the product of four adjacent "spins" around the smallest closed loop in the lattice. This is the gauge theory equivalent of the conventional Ising model, where the energy would involve the lattice average of the product of two adjacent spins.

For the actual evaluation we now simulate on a computer the $N_\sigma^3 \times N_\tau$ lattice, choosing for convenience $\xi = a_\sigma/a_\tau = 1$. For a given g, we place on each link a specific SU(N) matrix U, taking for example all $U = 1$ (ordered or "cold" start), or randomly distributed U's (disordered or "hot" start). Proceeding from this initial configuration, we then assign to every link of the lattice step by step a new matrix U', randomly chosen with the weight $S_G(U)$. After sufficiently many sweeps through the lattice ("iterations"), the plaquette averages stabilize to give $\bar{P}_\sigma$ and $\bar{P}_\tau$ at the chosen value of g. Using the renormalization group relation (Equation 26), we have the corresponding temperature—if the chosen g is sufficiently small for this relation to be applicable.

In Figure 1, we show the energy density thus obtained for the SU(2) system, based on calculations using a $10^3 \times 3$ lattice (13); here ε is normalized to the ideal gas limit

$$\varepsilon_{SB} = (3\pi^2/15)T^4. \qquad 32.$$

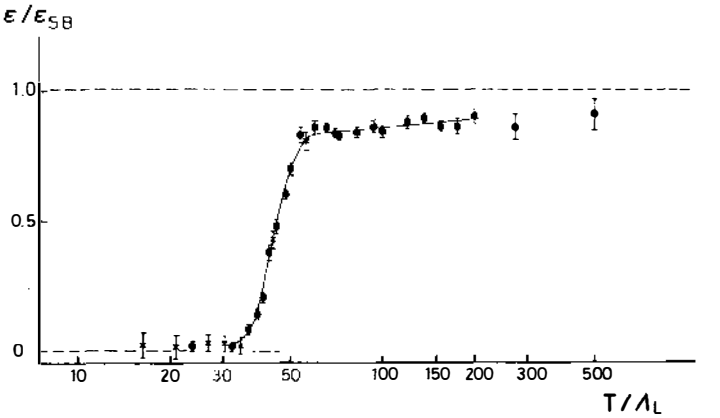

Figure 1 The energy density ε of the SU(2) gauge field system, normalized to its ideal gas limit ε_{SB}; from (13), on a $10^3 \times 3$ lattice.

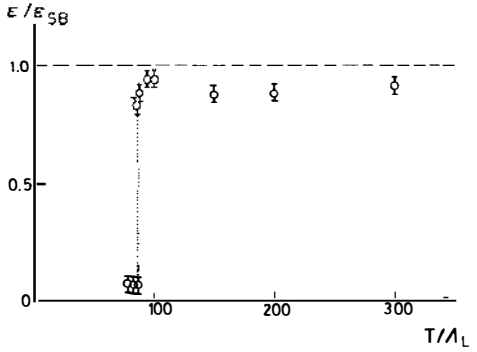

Figure 2 The energy density ε of the SU(3) gauge field system, normalized to its ideal gas limit ε_{SB}; from (37), on an $8^3 \times 3$ lattice.

At high temperatures, the system is seen to behave essentially like a gas of noninteracting gluons. Around $T = 40\Lambda_L$, there is a sudden drop in ε, and below this temperature, the behavior of the system agrees reasonably well with that of an ideal gas of gluonium states of mass $m_G \approx 1$ GeV (36). In Figure 2, the corresponding result is shown for the physically more interesting SU(3) case, evaluated on an $8^3 \times 3$ lattice (37). The behavior is quite similar, but the transition now occurs at $T \approx 80\Lambda_L$ and is discontinuous.

We noted above that the lattice scale Λ_L is arbitrary. If we take in each case results for the string tension σ at a comparable value of g (10, 38) and use the physical value $\sqrt{\sigma} \approx 400$ MeV, then both the SU(2) and the SU(3) system undergo the transition around

$$T_c \approx 150\text{–}200 \text{ MeV}. \qquad 33.$$

To assure that the change of behavior exhibited by ε is indeed due to the deconfinement transition, a corresponding order parameter is needed. It is obtained by noting that the lattice action (Equation 29) possesses a global symmetry under the center Z_N of the SU(N) gauge group (9a,b). The specific state, in which the system finds itself, may spontaneously break this symmetry, just as the ordered phase of the Ising model breaks the global Z_2 symmetry of its Hamiltonian. We are thus looking for the gauge theory analogue of the spontaneous magnetization. It is given (11, 12) by the average of the Polyakov loop

$$L_{\mathbf{x}}(U) = \frac{1}{N} \operatorname{Tr} \prod_{\tau=1}^{N} U_{\mathbf{x};\tau,\tau+1}, \qquad 34.$$

consisting of the product of all the U's in the temperature direction taken at a given spatial site $\mathbf{x}$. This product becomes a closed loop and thus gauge invariant by the periodicity condition (Equation 14). While S_G is invariant

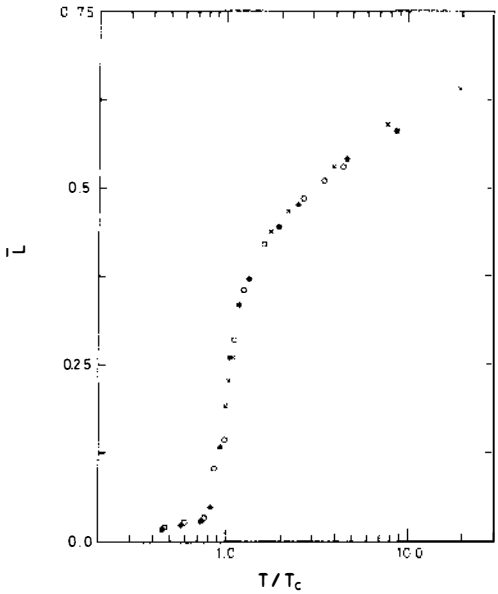

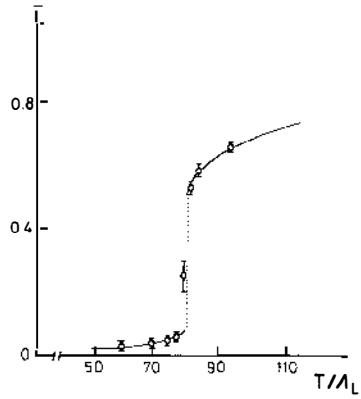

Figure 3 (*Left*) The deconfinement order parameter $\bar{L}$ of the SU(2) gauge field system, as function of T/T_c, with $T_c = 43\,\Lambda_L$; from (32), on a $10^3 \times 3$ lattice, using different actions.

Figure 4 (*Right*) The deconfinement order parameter $\bar{L}$ of the SU(3) gauge field system; from (39), on an $8^3 \times 2$ lattice.

under global Z_N transformations, the average $\bar{L}$, taken over the lattice and over configurations, acquires a factor $\exp(2r\pi i/N)$, with $0 \leq r \leq N-1$, and thus serves as an indicator for spontaneous symmetry breaking: it is zero for Z_N-symmetric states and nonzero if this symmetry is broken. The physical content of the change in symmetry becomes evident by noting that $\bar{L}$ measures the free energy F of a static quark (11, 12):

$$\bar{L} \sim e^{-F/T}. \qquad 35.$$

In the confinement regime, $F = \infty$ and hence $\bar{L} = 0$. Once color screening becomes effective, F becomes finite and hence $\bar{L}$ nonzero.[1] The transition from the confined to the deconfined state of the SU(N) gauge system is thus characterized by the spontaneous breaking of the global center Z_N symmetry.

In Figures 3 and 4 we show lattice results for $\bar{L}$ (32, 39). It thus is clear that

[1] This is true provided we remain in the same Z_N phase throughout, which we choose to be the one with $r = 0$.

the transition seen in the energy density behavior is indeed due to deconfinement. The nonzero values of $\bar{L}$ in the confinement regime observed in Figures 3 and 4 are finite lattice size effects (40). The abrupt change of ε in Figure 2 and that of $\bar{L}$ in Figure 4 suggest that the transition is of first order for the SU(3) system; more detailed studies confirm this (39, 41). The continuous behavior of both ε and $\bar{L}$ for the SU(2) system, on the other hand, points toward a higher order transition.

This difference in critical behavior for SU(2) and SU(3) gauge systems is in accord with a universality conjecture relating spin and gauge systems (42, 43). By integrating out all degrees of freedom in the partition function (Equation 28) except for the Polyakov loops (Equation 34) on all sites, one obtains from SU(N) gauge theory a system structurally equivalent to a Z_N spin theory of the same spatial dimensionality. As a result, we expect these theories to show the same critical behavior, and in fact Z_3 spin theory (the Potts model) has a discontinuous order/disorder transition (44), while that of the Z_2 spin theory (the Ising model) is continuous. More specifically, the critical exponents for the deconfinement transition in SU(2) gauge theory and for the order/disorder transition of the Ising model appear to agree (45), as would be expected if the two theories belong to the same universality class.

Before concluding our survey of gauge field thermodynamics, we want to consider the reliability of the lattice evaluation. The lattice regularization cuts out low and high momenta, which affects even a noninteracting system. This problem can, however, be controlled by comparing gauge theory results with those for an ideal gas evaluated on a lattice of the same size (46). The crucial question is whether the coupling values g used in the actual evaluation are sufficiently small to permit the use of the renormalization group relation (Equation 26). This would assure us that the results obtained correspond to the continuum limit of the theory. In Figure 5 we see a compilation of transition temperature and string tension data for the SU(3) gauge systems (24), shown as function of $6/g^2$. There are clear deviations from scaling, which requires that T_c and σ not depend on g; it appears possible that the asymptotic form (Equation 26) is valid for $g^2 \lesssim 1$. Even at larger couplings, however, one finds that dimensionless ratios, such as $T_c/\sqrt{\sigma}$ in Figure 5, are independent of g. We thus conclude that the lattice results obtained so far are a very promising beginning, but that calculations on larger lattices, combined with finite-size-scaling considerations (47), are certainly necessary.

QCD Thermodynamics with Quarks

The extension of SU(N) gauge field thermodynamics to include matter fields has two fundamental consequences.

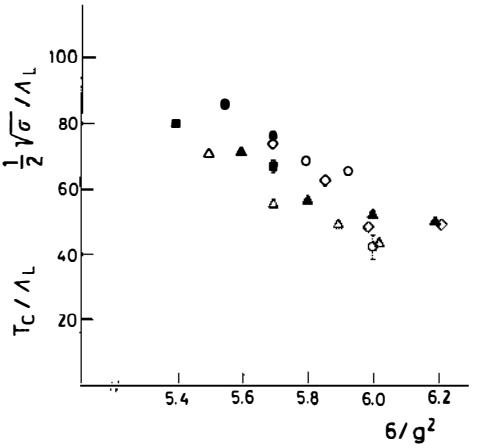

Figure 5 Present lattice results for the deconfinement temperature (*solid and open circles, diamonds*) and the string tension (*solid and open squares, triangles*), both as function of the inverse coupling $6/g^2$; from the compilation in (24).

The presence of the quark term in the Lagrangian (Equation 1) breaks the global invariance under the center of the gauge group (e.g. 48), which holds for the pure gluon system. The physical basis for this effect was already noted in a previous section; for $T > 0$, the color conductivity, just like the electric conductivity, does not vanish identically but is only exponentially small. With the global center symmetry broken, the average Polyakov loop $\bar{L}$ will also remain finite for all $T > 0$. The distinction between the confinement and deconfinement regimes thus becomes somewhat more qualitative in nature (9b, 16, 49).

The second new feature to appear is chiral symmetry. The Lagrangian (Equation 1) is invariant under the chiral transformation

$$\psi \to \psi' = \gamma_5 \psi, \qquad 36.$$

where γ_5 is the pseudoscalar Dirac matrix, because it contains only the chirally invariant spinor forms $\bar{\psi}\gamma_\mu\psi$. This invariance would be broken by adding the quark mass term (Equation 3), since $\bar{\psi}\psi$ is not invariant under the transformation in Equation 36. Even for $m_f = 0$, however, chiral invariance may be broken spontaneously; this would correspond to the spontaneous generation of an "effective" quark mass. Since the conduction electrons in a metal acquire an effective mass different from their mass value in vacuum, we may expect such a mass shift here as well. In the confinement regime, chiral symmetry is indeed broken, which leads to constituent quarks with an effective mass of about 300 MeV (for u and d quarks). In the deconfined plasma at high temperature, the quarks become massless again and hence chiral symmetry is restored. In the presence of massless matter fields, statistical QCD thus leads to another transition, from broken to restored chiral symmetry.

What is the relation between deconfinement and chiral symmetry restoration? At present, this question has no really satisfactory answer. There are good arguments that if the two phenomena are distinct, then deconfinement must occur at the lower temperature (50, 51): in general, confining potentials will break chiral symmetry. It may well be, however, that with the global Z_N symmetry broken by the introduction of light quarks, the chiral transition becomes the basic mechanism making deconfinement a genuine phase transition (52).

To obtain for the full partition function (Equation 16) a form suitable for computer simulation, one must integrate over the anticommuting spinor fields. This gives (53)

$$Z(N_\sigma, N_\tau, g) = \int \prod_{\text{links}} \mathrm{d}U \exp[-S_G(U)] [\det Q(U)]^{N_f}, \qquad 37.$$

where

$$Q(U) = [1 - \kappa M(U)] \qquad 38.$$

denotes the fermion matrix in Equation 21. As it connects $\bar{\psi}$ and ψ over the entire lattice, it is of dimension $(12N_\sigma^3 N_\tau) \times (12N_\sigma^3 N_\tau)$. The evaluation of the determinant of this very large matrix poses at present the main technical problem in the numerical evaluation. For reasonable lattice sizes, it has up to now been carried out only in several approximation schemes:

1. In the hopping-parameter expansion (54, 55)

$$\ln \det(1 - \kappa M) = -\mathrm{Tr} \sum_{l=1}^{\infty} \frac{\kappa^l}{l} M^l, \qquad 39.$$

only the first few leading terms are generally retained for the actual evaluation.

2. In the pseudo-fermion method (56), the quark determinant is written as the integral over complex scalar fields Φ and $\bar{\Phi}$

$$(\det Q)^{-1} = \int \prod_{\text{sites}} \mathrm{d}\Phi \, \mathrm{d}\bar{\Phi} \exp[-(\bar{\Phi} Q \Phi)], \qquad 40.$$

which must then be evaluated by a separate Monte Carlo simulation for each configuration of U's.

3. In the microcanonical approach (57), one considers an artificial classical system that is integrable and leads to the partition function (Equation 37). Solving the equations of motion for this system by methods from molecular dynamics, one can then replace the ensemble average (Equation 37) by the corresponding time average, provided ergodicity holds.

The next generation of supercomputers, both faster and with a much larger memory than those employed today, may perhaps bring a precise evaluation within reach. In any case, it is reassuring that all the results obtained so far agree quite well both qualitatively and quantitatively, even though the evaluation schemes differ considerably. In Table 1 we list the calculations carried out up to the end of 1984, indicating both the type of quark action and the fermion determinant scheme used. All find a sudden change in the energy density ε, in $\bar{L}$ as a measure of confinement, and in the average of $\bar{\psi}\psi$ as a measure of chiral symmetry. For a representative and perhaps most transparent case, we look at the results obtained using Wilson's form Equations 21 and 22 of the quark action, evaluated in the hopping-parameter expansion (Equation 39) (19).

For lattices of small temporal extension ($N_\tau \approx 3$–5), the partition function (Equation 37) then has the form

$$Z(N_\sigma, N_\tau, g) = \int \prod_{\text{links}} dU \exp[-S_{\text{eff}}(U)], \qquad 41.$$

with

$$S_{\text{eff}}(U) \approx S_G(U) - 4N_f(2\kappa)^{N_\tau} \sum_{\text{sites}} \text{Re } L \qquad 42.$$

denoting the effective action in lowest order hopping-parameter expansion. Only closed loops contribute to S_{eff}, and for small N_τ the dominant contributions are those from Polyakov loops. We note that the action (Equation 41) has the structure of a gauge-invariant spin system in an effective external field (9b, 49, 61), whose strength is $4N_f(2\kappa)^{N_\tau}$. For infinitely heavy ("static") quarks, κ vanishes and we recover the pure gauge theory, with $\bar{L} = 0$ in the confinement regime. For finite quark masses ("dynamic" quarks), κ is finite and the external field nonzero; it breaks the global Z_N symmetry and hence makes $\bar{L} \neq 0$ even when we have confinement. This is how the "ionization" mechanism of local hadron production, discussed above, enters the generalized spin picture.

Table 1 Critical parameters in different fermion schemes

Scheme	N_τ	N_f	$6/g_c^2$	T_c/Λ_L^0	Ref.
Wilson κ^4	3	2	5.30 ± 0.05	131 ± 8	19
Wilson κ^5	3	2	5.25 ± 0.05	123 ± 8	19
Kogut-Susskind, canonical	4	3	5.3	100	58
Kogut-Susskind, canonical	2	2	4.6	89	59
Kogut-Susskind, microcanonical	4	4	5.1	106	60

The energy density of the quark-gluon system has the form

$$\varepsilon = \varepsilon_G + \varepsilon_Q; \qquad 43.$$

the gluonic contribution ε_G is again given by Equation 30, but the plaquette averages are now calculated with the effective action (Equation 41) instead of the pure gluon form (Equation 29). The quark contribution in the lowest order hopping-parameter expansion is given by

$$\varepsilon_Q/T^4 \approx 3N_\tau^3 N_f (2\kappa)^{N_\tau} \text{ Re } \bar{L}. \qquad 44.$$

The presence of dynamic quarks thus leads to a partial gauge field alignment in an effective external field, and ε_Q measures the degree of this alignment.

In Figure 6, we show the resulting overall energy density calculated on an $8^3 \times 3$ lattice (19), including terms up to κ^4 in the hopping-parameter expansion. The relation between κ and g is given by Equation 25, that between g and a by Equation 26; we consider the case of two quark flavors. The energy density of the interacting system is again compared to the noninteracting gas limit ε_{SB} on a lattice of the same size; also shown is the behavior of an ideal gas of π, ρ, and ω mesons in all their possible charge and spin states. We see that the system at low temperature behaves like a meson gas; around $T/\Lambda_L \approx 150$ it undergoes a sudden transition, and above that

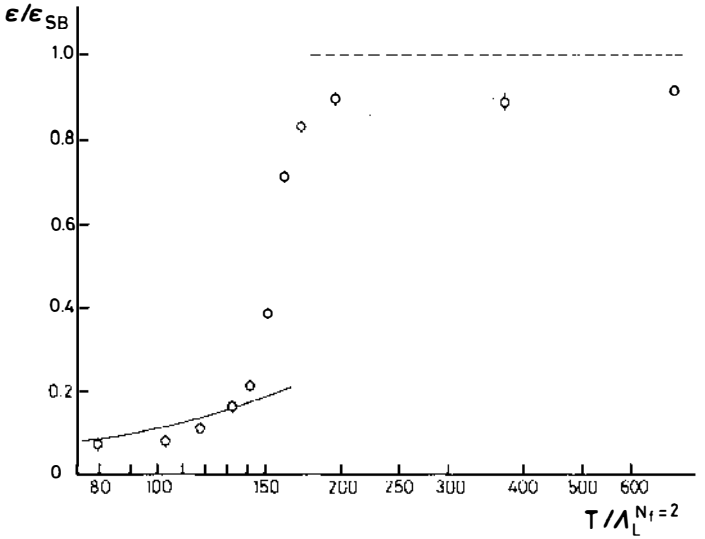

Figure 6 The energy density in QCD with dynamic quarks, evaluated in hopping-parameter expansion; from (19), on an $8^3 \times 3$ lattice. The solid curve corresponds to an ideal meson gas (π, ρ, ω).

temperature it approaches the ideal gas limit. The deconfinment measure $\bar{L}$ parallels this behavior, as seen in Figure 7; note that with Equation 26, $6/g^2 \approx 5.3$ corresponds to $T/\Lambda_L \approx 150$. We can thus again associate the transition with deconfinement. It should be noted that while $\bar{L}$ is nonvanishing in the confined regime, in accord with the broken Z_N symmetry due to the presence of dynamic quarks, it is, however, quite small there. This agrees with the arguments (9b, 19) presented above, suggesting at most a small symmetry breaking.

As $\bar{\psi}\psi$ is not invariant under the chiral transformation (Equation 36), it provides an order parameter for chiral symmetry restoration. In lowest order hopping-parameter expansion, the lattice average of $\bar{\psi}\psi$ takes the form

$$\langle\bar{\psi}\psi\rangle/T^3 \sim (1 - \mathrm{Re}\ \bar{L}), \qquad 45.$$

so that chiral symmetry is broken in the deconfinement region, where $\bar{L}$ is small; it is restored as $\bar{L}$ approaches the ideal gas limit of unity. From Equation 42, it is clear that in this approximation the transition points for deconfinement and chiral symmetry restoration coincide. In Wilson's formulation for quarks on the lattice, however, the study of chiral symmetry restoration is not without problems. As was already mentioned, the spurious mass states are removed by making them very massive. It is therefore particularly important to check the transition points for the two

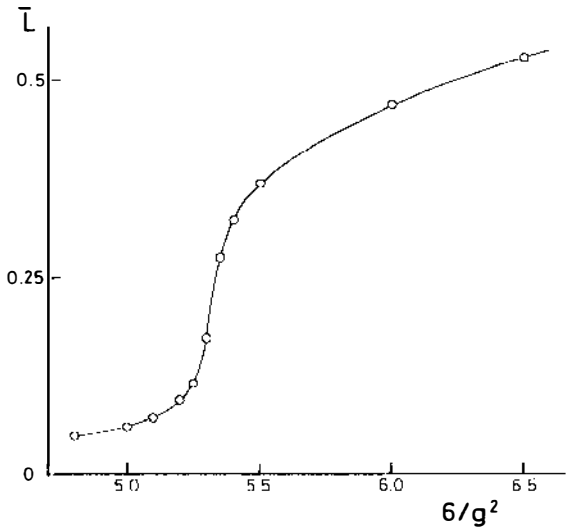

Figure 7 The deconfinement measure $\bar{L}$ in QCD with dynamic quarks, evaluated in hopping-parameter expansion; from (19), on an $8^3 \times 3$ lattice.

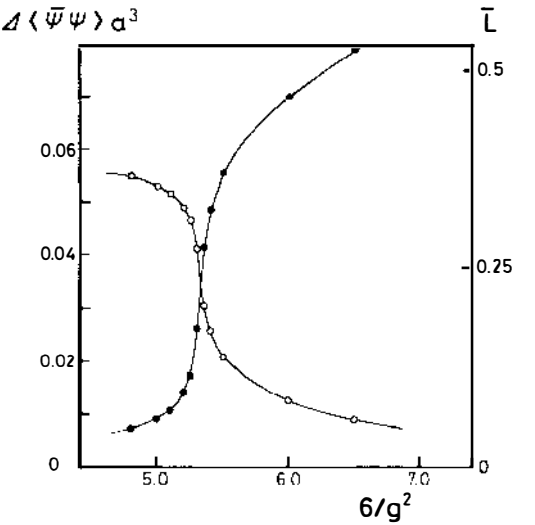

Figure 8 Deconfinement measure $\bar{L}$ and chiral symmetry measure $\langle\bar{\psi}\psi\rangle$, evaluated in hopping-parameter expansion; from (19), on an $8^3 \times 3$ lattice.

transition phenomena in other formulations as well. We show in Figures 8 and 9 a comparison of $\bar{L}$ and $\langle\bar{\psi}\psi\rangle/T^3$ for Wilson quarks in the hopping-parameter expansion (19) and for Kogut-Susskind quarks in the micro-canonical approach (60): they agree very well, and still further calculations (58, 59) confirm this. It thus appears that deconfinement and chiral symmetry restoration in statistical QCD at vanishing baryon number density occur indeed at the same temperature. A further clarification of the

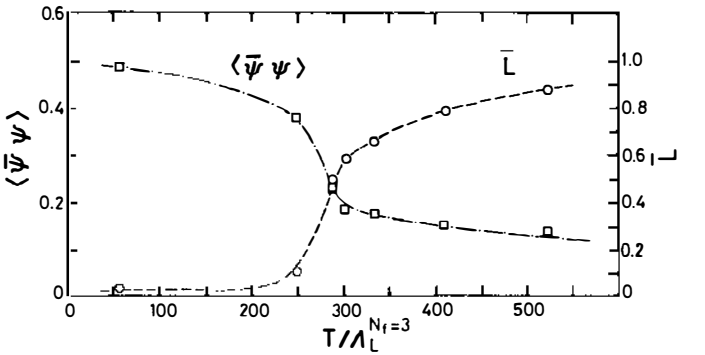

Figure 9 Deconfinement measure $\bar{L}$ and chiral symmetry measure $\langle\bar{\psi}\psi\rangle$, evaluated in the microcanonical approach; from (60), on an $8^3 \times 4$ lattice.

relation between these phenomena is an interesting challenge in statistical QCD.

To conclude this section, we turn to the question of the actual value of the deconfinement temperature. In Table 1, we list the values of T_c obtained in the different approaches; for purposes of comparison, they are all converted into the units of Λ_L for the zero-flavor case. The results of the hopping-parameter expansion are expected to be slightly higher, as the quark masses are not yet very small, when we use Equation 25. Bearing that in mind, we see that deconfinement occurs roughly at

$$T_c/\Lambda_L^0 \approx 100, \qquad 46.$$

to be compared with the value $T_c/\Lambda_L^0 \approx 80$ for pure gauge field thermodynamics on lattices of similar size. For a reliable conversion of this into physical units, we must wait until the evaluation of the hadron spectrum with dynamic quarks is completed (15). At present, the use of available data from comparable lattices gives

$$T_c \approx (200\text{–}250)\ \text{MeV} \qquad 47.$$

as the most reasonable value.

OUTLOOK

Dense Baryonic Matter

Statistical quantum chromodynamics predicts, as we have seen, a deconfinement transition for strongly interacting matter of vanishing overall baryon number density. In a meson gas, color screening dissolves with increasing temperature the binding between quarks and antiquarks, transforming the system into a chromoplasma of unconfined colored constituents. The decisive element in the screening mechanism is the increase of color charge density, which is here achieved by an increase of temperature resulting in particle production. Matter at high density can, however, also be formed by compressing a system of many nucleons at low temperature; this leads to a high density of baryons and hence also of quarks.

The complete phase diagram of strongly interacting matter must thus describe the phase structure as a function of the temperature T *and* the baryon number density n_B or the corresponding baryonic "chemical" potential μ_B. So far, quantitative predictions from QCD exist only for $\mu_B = 0$. Extending these results to nonzero baryon densities is obviously one of the most urgent problems to be addressed by statistical QCD. The partition function (Equation 10) then becomes more generally

$$Z(T, \mu_B, V) = \text{Tr}\ \{\exp[-\beta(H - \mu N_B]\}, \qquad 48.$$

with N_B denoting the operator for the overall baryon number. Only the first steps toward a viable lattice evaluation have yet been taken (62–65).

In Figure 10, we show a possible schematic phase diagram for strongly interacting matter, which at $\mu_B = 0$ agrees with the results of the previous section. The coincidence of deconfinement and chiral symmetry restoration in that case does not imply similar behavior for $T = 0$ as a function of μ_B. When, in a Mott transition, Debye screening dissolves the local binding between charges, this does not necessarily mean that a state of completely unbound constituents is the energetically most favorable one. Even beyond the transition point, collective binding mechanisms are still possible. The Cooper pairs in superconducting materials provide an example of a such bound state; they can, however, exist only at very low temperatures because thermal motion quickly overcomes the binding force. Something similar could, at least in principle, also occur in strongly interacting matter at low temperature: beyond the deconfinement point, chiral symmetry could still be broken, thus providing us with a system of massive colored quarks as constituents. Increasing either the temperature or the baryonic chemical potential would convert this stage into the true chromoplasma of massless colored quarks and gluons. Statistical QCD will eventually tell us if such an intermediate phase—something like a color superconductor—really exists. For the time being, the question is completely open.

Deconfinement and Nuclear Collisions

To conclude our survey, we take a short look at the possibility of creating dense strongly interacting matter in the laboratory. For this, the collision of heavy nuclei seems to be our only, certaintly not perfect, tool.

When two energetic hadrons undergo a central collision, they essentially pass through each other, leaving behind a streak of energy deposited in a certain space-time region. This energy subsequently decays into the observed hadronic secondaries. In a typical proton-proton collision, the energy deposited is about 0.3 GeV fm^{-3}. For the formation of the quark-gluon plasma, we need at least 2.5 GeV fm^{-3}, since $\varepsilon/T^4 \approx 12$ and $T_c \approx 200$

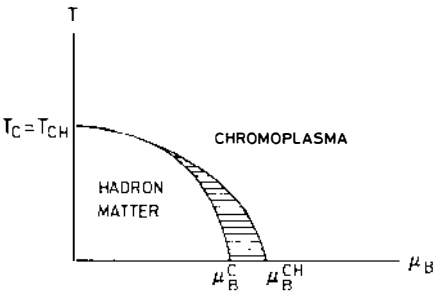

Figure 10 Schematic view of a possible phase diagram in QCD, as function of temperature T and baryonic chemical potential μ_B.

MeV. The typical energy deposit achieved in a collision of two identical nuclei of mass number A is expected (24) to be about (1–3) $A^{1/3}$ GeV fm^{-3}; for heavy nuclei, this is well above the critical value. This estimate assumes a constant deposit per unit rapidity and hence becomes independent of the collision energy.

A sufficient local energy deposit does not, of course, guarantee the applicability of equilibrium thermodynamics to the process. The volume of space-time in question here is far from infinite. It is therefore crucial that the mean free path of quarks and gluons in the resulting medium be sufficiently small in comparison to the size of the system. Only then can we expect a description in terms of an expanding plasma with a subsequent transition to hadronic matter to be meaningful.

Assuming that in energetic nuclear collisions there is indeed plasma formation, how can we verify this experimentally? The discussion of signatures has so far not led to any unambiguous test, but rather to a number of supporting predictions (66). Since photons, because of the comparatively weak electromagnetic interaction, can escape unmodified if produced in the primordial plasma, they should carry information about this state (67). The transverse momenta of hadronic secondaries act as a measure of the temperatures involved, and studying their dependence on initial energy density should produce evidence for the latent heat of deconfinement (68) depicted in Figures 2 and 6. Finally, if the initial plasma achieves an equilibrium even between the different quark flavors ("chemical equilibrium"), then the resulting flavor ratios should lead to observable consequences for the measured hadron ratios (69).

These and a variety of other aspects of plasma formation in nuclear collisions have been and are at present the subject of intensive studies. The interest they trigger is perhaps best explained by recalling the ultimate aim of this field of research: an understanding of the states of matter in strong interaction physics.

ACKNOWLEDGMENT

It is a pleasure to thank R. Baier, J. Engels, and B. Petersson for a critical reading of the manuscript.

Literature Cited

1. Kajantie, K., ed. *Quark Matter 1984*; Proc. 4th Int. Conf. on Ultra-Relativistic Nucleus-Nucleus Collisions. Berlin/Heidelberg/New York: Springer-Verlag (1985)
2. *RHIC and Quark Matter*; Proposal for a Relativistic Heavy Ion Collider at BNL, *Rep. BNL 51801*. Upton, NY: Brookhaven Natl. Lab. (1984)
3. Pomeranchuk, I. *Dokl. Akad. Nauk. SSSR* 78:889 (1951); Hagedorn, R. *Nuovo Cimento Suppl.* 3:147 (1965)

4. Morley, P. D., Kislinger, M. B. *Phys. Rep.* 51:63 (1979); Shuryak, E. V. *Phys. Rep.* 61:71 (1980)
5. Kapusta, J. *Nucl. Phys. B* 148:461 (1979)
6. Khalashnikov, O. K., Klimov, V. V. *Phys. Lett.* 88B:328 (1979)
7. Wilson, K. *Phys. Rev. D* 10:2445 (1974); Wilson, K. In *New Phenomena in Subnuclear Physics*, ed. A. Zichichi. New York: Plenum (1977)
8. Borgs, C., Seiler, E. *Nucl. Phys. B* 215: 125 (1983)

9a. Polyakov, A. M. *Phys. Lett.* 72B:477 (1978)

9b. Susskind, L. *Phys. Rev. D* 20:2610 (1979)

10. Creutz, M. *Phys. Rev. Lett.* 43:553 (1979); *Phys. Rev. D* 21:2308 (1980)
11. McLerran, L. D., Svetitsky, B. *Phys. Lett.* 98B:195 (1981); *Phys. Rev. D* 24:450 (1981)
12. Kuti, J., Polónyi, J., Szlachányi, K. *Phys. Lett.* 98B:199 (1981)
13. Engels, J., Karsch, F., Montvay, I., Satz, H. *Phys. Lett.* 101B:89 (1981); *Nucl. Phys. B* 205[FS5]:545 (1982)
14. Politzer, H. D. *Phys. Rep.* 14:129 (1974); Altarelli, G. *Phys. Rep.* 81:1 (1982)
15. Hasenfratz, A., Hasenfratz, P. *Ann. Rev. Nucl. Part. Sci.* 35:559 (1985)
16. Satz, H. *Nucl. Phys. A* 418:447c (1984)
17. Mott, N. F. *Rev. Mod. Phys.* 40:677 (1968) and references given there
18. Marciano, W., Pagels, H. *Phys. Rep.* 36:137 (1978); Wilczek, F. *Ann. Rev. Nucl. Part. Sci.* 32:177–209 (1982)
19. Çelik, T., Engels, J., Satz, H. *Nucl. Phys. B* 256:670 (1985)
20. Bernard, C. *Phys. Rev. D* 9:3312 (1974)
21. Wegner, F. J. *J. Math. Phys.* 10:2259 (1971)
22. Hasenfratz, A., Hasenfratz, P. *Nucl. Phys. B* 193:210 (1981)
23. Kawamoto, N. *Nucl. Phys. B* 190 [FS3]:617 (1981)
24. Satz, H. See Ref. 1
25. Villain, J. *J. Phys.* 36:581 (1975); Drouffe, M. *Phys. Rev. D* 18:1174 (1978)
26. Manton, N. S. *Phys. Lett.* 96B:328 (1980)
27. Bhanot, G., Creutz, M. *Phys. Rev. D* 24: 3212 (1981)
28. Christ, N. H., Friedberg, R., Lee, T. D. *Nucl. Phys. B* 10[FS6]:310 (1982)
29. Szymanzik, K. *Nucl. Phys. B* 226:187 (1983)
30. Kogut, J., Susskind, L. *Phys. Rev. D* 11:395 (1975); Susskind, L. *Phys. Rev. D* 16:3031 (1977)
31. Drell, S. D., Weinstein, M., Yankielowicz, S. *Phys. Rev. D* 14:487 (1976)
32. Gavai, R. V., Karsch, F., Satz, H. *Nucl. Phys. B* 220[FS8]:223 (1983)
33. Nielsen, H. B., Ninomiya, M. *Nucl. Phys. B* 185:20 (1981)
34. Binder, K., ed. *Monte Carlo Methods in Statistical Physics.* Berlin/Heidelberg/ New York: Springer-Verlag (1979)
35. Karsch, F. *Nucl. Phys. B* 205[FS5]:285 (1982)
36. Engels, J., Karsch, F., Satz, H. *Phys. Lett.* 102B:332 (1981)
37. Çelik, T., Engels, J., Satz, H. *Phys. Lett.* 129B:323 (1983)
38. Bhanot, G., Rebbi, C. *Nucl. Phys. B* 180[FS2]:469 (1981); Gutbrod, F., Hasenfratz, P., Kunszt, Z., Montvay, I. *Phys. Lett.* 128B:415 (1983)
39. Kogut, J., et al. *Phys. Rev. Lett.* 50:393 (1983)
40. Çelik, T., Engels, J., Satz, H. *Z. Phys. C* 22:301 (1984)
41. Çelik, T., Engels, J., Satz, H. *Phys. Lett.* 125B:411 (1983)
42. Polónyi, J., Szlachányi, K. *Phys. Lett.* 110B:395 (1982)
43. Svetitsky, B., Yaffe, L. G. *Nucl. Phys. B* 210[FS6]:423 (1982)
44. Blöte, H. W. J., Swendsen, R. H. *Phys. Rev. Lett.* 43:799 (1979); Knak Jensen, S. J., Mouritsen, O. G. *Phys. Rev. Lett.* 43:1736 (1979)
45. Gavai, R. V., Satz, H. *Phys. Lett.* 145B: 248 (1984)
46. Engels, J., Karsch, F., Satz, H. *Nucl. Phys. B* 205[FS5]:239 (1982)
47. Kennedy, A. D., Kuti, J., Meyer, S., Pendleton, B. *Phys. Rev. Lett.* 54:87 (1985)
48. Çelik, T., Engels, J., Satz, H. *Phys. Lett.* 133B:427 (1983)
49. Banks, T., Ukawa, A. *Nucl. Phys. B* 225[FS9]:145 (1983)
50. Shuryak, E. V. *Phys. Lett.* 107B:103 (1981); *Nucl. Phys. B* 203:140 (1982)
51. Pisarski, R. D. *Phys. Lett.* 110B:155 (1982)
52. Alessandrini, V. *Orsay Rep.* LPTHE 84/14 (1984)
53. Mathews, T., Salam, A. *Nuovo Cimento* 12:563 (1954)
54. Lang, C. B., Nicolai, H. *Nucl. Phys. B* 200[FS4]:135 (1982)
55. Hasenfratz, A., Hasenfratz, P., Kunszt, Z., Lang, C. B. *Phys. Lett.* 110B:289 (1982)
56. Fucito, F., Marinari, E., Parisi, G., Rebbi, C. *Nucl. Phys. B* 180[FS2]:369 (1981)
57. Polónyi, J., Wyld, H. W. *Phys. Rev. Lett.* 51:2257 (1983)
58. Fucito, F., Solomon, S. *Cal. Tech. Rep.* CALT-68-1084 (1984); Fucito, F., Rebbi, C., Solomon, S. *Cal. Tech. Rep.* CALT-68-1127 (1984)
59. Gavai, R. V., Lev, M., Petersson, B. *Phys. Lett.* 140B:397 (1984); 149B:492 (1984)

60. Polónyi, J., Wyld, H. W., Kogut, J. B., Shigemitsu, J., Sinclair, D. K. *Phys. Rev. Lett.* 53:644 (1984)
61. Hasenfratz, P., Karsch, F., Stamatescu, I. O. *Phys. Lett.* 133B:211 (1983)
62. Hasenfratz, P., Karsch, F. *Phys. Lett.* 125B:308 (1983)
63. Kogut, J., et al. *Nucl. Phys. B* 225:93 (1983)
64. Gavai, R. V., Ostendorf, A. *Phys. Lett.* 132B:137 (1983)
65. Bilić, N., Gavai, R. V. *Z. Phys. C* 23:77 (1984)
66. Gyulassy, M. *Nucl. Phys. A* 418:59c (1984); Cleymans, J., Gavai, R. V., Suhonen, E. *Phys. Rep.* In press (1985)
67. Shuryak, E. V. *Sov. J. Nucl. Phys.* 28:408 (1978); Kajantie, K., Miettinen, H. I. *Z. Phys. C* 9:341 (1981); 14:357 (1982)
68. Van Hove, L. *Phys. Lett.* 118B:138 (1982)
69. Rafelski, J. *Nucl. Phys. A* 418:215c (1984)